HYBRID VOLUMETRIC RECONSTRUCTION: WATERSHED AND DEFORMABLE BALLOON-SIMPLEX MESHES

EL FAZAZY KHALID, SATORI KHALID

LIIAN Laboratory - Faculty of Sciences 30000 Fez – MOROCCO

ABSTRACT

Extracting three-dimensional objects from volume data, with previous techniques, were based on stitching a series of two-dimensional contours together or connecting two-dimensional contours using surface interpolation. Deformable simplex meshes DSM proposes an original surface representation to recover 3D object boundaries and treats data set as a complete volume as opposed to a series of slices. However, it requires that object of interest has been previously isolated from the other objects and the result of reconstruction depends on the interaction process between segmentation and interpolation. Moreover, as like as deformable models, it reveal poor convergence to concave boundaries and require initialization.

In this paper, we propose to solve the problem resulting from the internal force formulation by adding a balloon force. Then, we combine the improved deformable simplex meshes (DSM-Balloon) with watershed method. The segmentation strategy is to use the segmentation result of watershed as prior information for DSM-Balloon. On one hand, the watershed prepares the initial lines for the DSM-Balloon which ensures automatic initialization and simplex meshes convergence. On other hand, the result of DSM-Balloon will overcome the over-segmentation and smoothing problem of watershed.

Keywords: *Hybrid Reconstruction, Deformable Simplex Meshes, Watershed, Balloon Force, 3D Medical Objects.*

1. INTRODUCTION

The incorporation of priori information as shape, dimension, position and orientation of an object in the process of segmentation improve the efficiency and the accurateness of segmentation. Indeed, deformable models are a satisfactory solution that incorporates prior information in order to extract an object. While initializing coarsely a contour, it is possible to deform it so that it positioned itself on the boundaries of the object of interest. Generally, there are two types of deformable models: the parametric deformable models [1] and geodesic deformable models [2, 3]. The parametric deformable model "snake" has a considerable attention since its first introduction by Kass, Witkin, and Terzopoulus [1]. All properties and behaviors of parametric deformable models are specified through an energy function. A partial differential equation pushes the deformable model to evolve and reduce its energy, so that the local minimums of this energy correspond to the properties of the required image. The parametric deformable models have been used in a range of applications, including boundaries detection [1], object recognition [4, 5], shape modeling [5, 6], and movement tracking [4, 7]. The geometric deformable models were proposed simultaneously by Caselles et al. [3] and by Malladi et al. [2], to address topological change of parametric contours. However, due to calculating complexity and a slower speed convergence, the model require several times reset.

3D medical image segmentation slice by slice, while applying 2D deformable models, is a process requiring post-treatments to reconnect the sequence of the 2D contours in a continuous surface. Indeed, the 3D deformable surface is a robust segmentation technique that assures a global smoothing and a consistency between slices of 3D image. It treats data set as a complete volume as opposed to a series of slices. 3D medical object reconstruction can be achieved using the general algorithm of Delingette based on simplex meshes [8]. One of deformable simplex meshes advantages is that deformation process can be executed in a simple and efficient manner. However, internal energy formulation presents an inconvenient that decreases the boundaries extraction accurateness. Moreover, as

like as deformable models, it reveal poor convergence to concave boundaries and require initialization.

The remainder of this paper is organized as follows: in the section 2, we review the essential mathematical jargon and the fundamental features of the DSM to inspire its interest to the segmentation problems. The section 3, focus on problem statement. In section 4, we present our contribution to improve the results of DSM to reconstruct valid object boundaries. The emphasis will be on properties and the rules used to build our combinatorial approach. Then, section (5 and 6) provide results, summarize the proposed method and points out our future research.

2. SIMPLEX MESHES

The simplex meshes have a constant connectivity. The main geometric of simplex mesh consists of a simple representation by giving the position of a vertex relatively to its neighbors. To represent three-dimensional surface, one uses the 2- simplex meshes where each vertex is connected to three neighboring vertices. The structure of simplexes meshes is dual to the structure of triangulation.

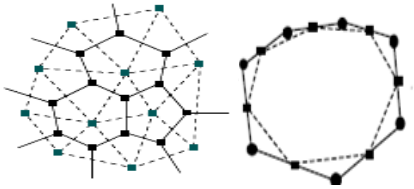

Fig.1: duality between triangulations and 2-simplex meshes (Lift) and 1-simplex meshes (right).

2.1 Geometry of 2-simplex meshes

The coordinates of $P_{(i)}$ are defined relatively to its neighbors:

$$P_i = \sum_{k=1}^{3} \varepsilon_{k(i)} P_{N\,k(i)} + L(r_i, d_i, \varphi_i) n_i \qquad (1)$$

$d_{(i)}$ is the distance between $P^{\perp}{}_{(i)}$ and centre $C_{(i)}$.

$$L(r_i, d_i, \varphi_i) = \frac{\left(r_i^2 - d_i^2\right)\tan(\varphi_i)}{\varepsilon\sqrt{r_i^2 + \left(r_i^2 - d_i^2\right)\tan^2(\varphi_i)} + r_i} \quad (2)$$

$\varepsilon = 1$ *if* $|\varphi i| < \pi/2$

$\varepsilon = -1$ *if* $|\varphi i| > \pi/2$

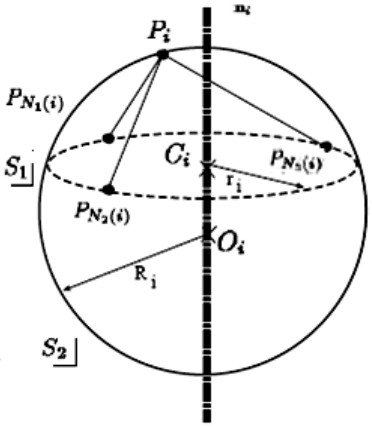

Fig. 2: The circle S_1 *of center* $C_{(i)}$ *and ray* $r_{(i)}$ *circumscribes the vertices* $(P_{N1(i)}; P_{N2(i)}; P_{N3(i)})$. *The sphere* S_2 *of center* $O_{(i)}$ *and ray* $R_{(i)}$ *circumscribes the four vertices* $(P_{(i)}; P_{N1(i)}; P_{N2(i)}; P_{N3(i)})$.

The metric parameters $(\varepsilon_{1i}\ ; \varepsilon_{2i}\ ; \varepsilon_{3i})$ at a vertex P_i are the barycentric coordinates of the orthogonal projection $P_i^{\perp}$ of P_i onto the neighboring triangle $(P_{N1(i)}; P_{N2(i)}; P_{N3(i)})$.

$$P^{\perp}{}_{(i)} = \sum_{k=1}^{3} \varepsilon_{k(i)} P_{N\,k(i)}$$

2.2 Deformation law of 2-simplex meshes

A deformable simplex meshes deforms under the combined action of a regularization (or internal) term and a data (or external) term enforcing the attraction of the surface towards object boundaries. In order to compute the evolution of the simplex mesh, the Newtonian law:

$$m\frac{d^2 P_i}{dt^2} = -\gamma\frac{dP_i}{dt} + F_{\text{int}} + F_{ext}$$

is discretized using central finite differences with an explicit scheme:

$$P_i^{t+1} = P_i^t + (1-\gamma)\left(P_i^t - P_i^{t-1}\right) + \alpha_i F_{\text{int}} + \beta_i F_{ext}$$

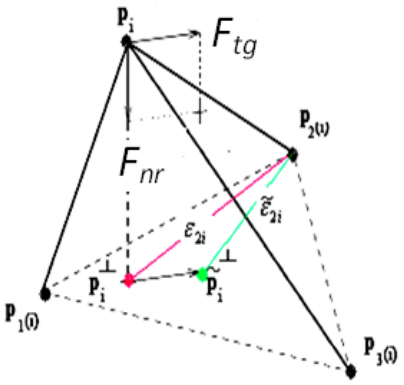

Fig. 3: the geometry and definition of regularizing force.

The internal force applied on vertex P_i is decomposed into a normal force and a tangential force. The goal of the tangential force is to control the vertex position with respect to its three neighbors in the tangent plane.

$$F_{tg} = \sum_{k=1}^{3} (\tilde{\varepsilon}_{k(i)} - \varepsilon_{k(i)}) P_{k(i)} \quad (5)$$

$\tilde{\varepsilon}_{k(i)}$ corresponding to the prescribed value of the metric parameters after deformation.

The goal of the normal force is to constrain the mean curvature of the surface through the simplex angle φ_i.

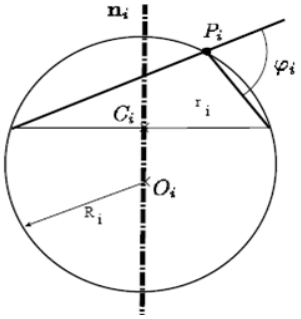

Fig. 4: Definition of simplex angle φ_i.

The general expression of the normal force is governed by the reference simplex angle $\tilde{\varphi}_i$:

$$F_{nr} = (L(r_i, d_i, \tilde{\varphi}_i) - L(r_i, d_i, \varphi_i)) n_i \quad (6)$$

Where L is the function (2) that controls the local mean curvature at P_i.

The expression of the external force is dependent on the nature of the dataset. On volumetric images, the gradient intensity is used for local deflection of the mesh towards the voxels of maximum variation of intensity. The edge information, on the other hand, corresponds to gradient maxima and entails larger deformations of the mesh. Generally, the gradient intensity and edge information are combined to compute external force:

$$F_{ext} = F_{Grad} + F_{Edge} \quad (7)$$

The Gradient force at vertex $P_{(i)}$ relies on the search in his neighborhood for the voxel of maximum gradient intensity. If V is the voxel containing, $P_{(i)}$, then we inspect around V for the voxel G_i of highest gradient intensity.

$$F_{Grad} = \beta_i^{Grad} ((G_i - P_i).n_i) n_i \quad (8)$$

The computation of the edge force at vertex $P_{(i)}$ consists in finding the closest edge voxel E_i in the normal direction n_i of the mesh. The maximum number of edge voxels scanned is determined as a percentage of the overall radius of the edge image.

$$F_{Edge} = \beta_i^{Edge} (E_i - P_i) \quad (9)$$

3. PROBLEM STATEMENT

One of the difficulties with DSM internal forces formulation is that the process of deformation is based on a constant connectivity between vertices which implies that the position of a vertex is affected by neighboring vertices deformation. Because the coordinates of P_i are computed relatively to its neighbors (1). Consequently, those interactions can push a number of vertices to left valid positions that fit conveniently the object boundaries and converge to the wrong position. Repeating the computation process for each vertex increases the likelihood of invalid missing data interpolation. Generally, we have noted two distinct behaviors of vertices during deformation: vertices that fit the object boundaries and those that pass from high gradient intensity to weak intensity values thus get over object boundaries.

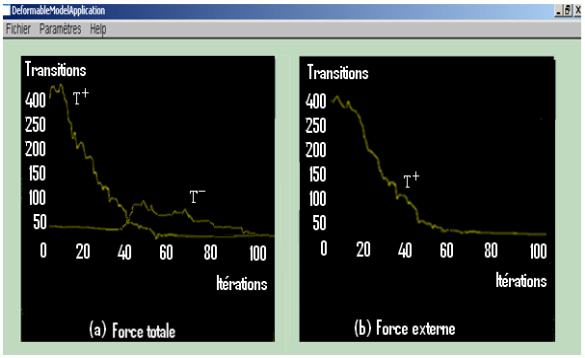

Fig. 5: DSM vertices transitions from voxels v_i^t to voxels v_i^{t+1} : (a) positive T^+ and negative T^- transitions caused by total force; (b) positive transitions caused by external force.

The solution proposed to address this problem is based on inflation force. Since DSM is initialized outside of object and the normal direction n_i is defined outside toward inside object (9), the mesh always deforms in the normal sense. And since we want to address the problem of negative vertices by bringing back and repositioning them again on the boundary, we define a new external force drifted from inflation force F_{ballon} proposed by Cohen [9].

$$F_{ext} = F_{Grad} + F_{ballon}$$

Indeed, we define a potential that permits "to inflate" or "to deflate" the mesh according to the normal sign κ :

$$F_{ballon} = \kappa.n_{(i)}\left(P_i - E_i\right)$$

The inflation force consists in finding the closest edge voxel E_i in the sense of mesh normal direction κ . However, while DSM-Balloon resolve vertices negative transitions, it reveals poor convergence to concave boundaries and require initialization. Indeed, it requires that object of interest has been previously isolated from other objects. To overcome those artifacts, in our previews contribution [10], we have combining DSM and watershed. The watershed transforms [13, 14, 15, 16, 17] reduce sensitivity to initialization and alleviate convergence problem. However, the result of watershed depends on the order in which pixels are treated during execution. Also, there are many issues concerning the accuracy of watershed lines and over-segmentation [11, 12].

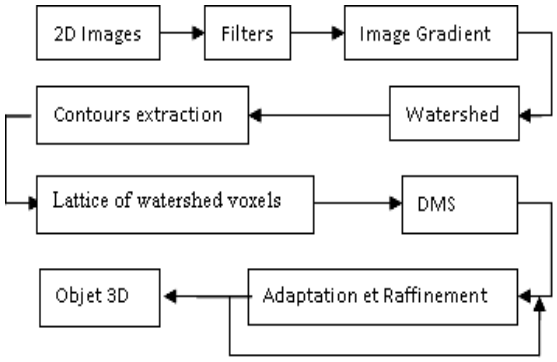

Fig. 6: combined DSM and watershed diagram.

However, the combination of DSM and watershed proposed in [10], don't address the problem of vertices negative transitions in a convenient way. Indeed, after first stages of deformation, the vertices P_i witch fit the watershed voxels are labeled with an index. Consequently, unlabelled vertices follow the same law of motion. Labeled vertices on simplex meshes are not deformable yet inside the watershed boundary. Though, while stopping the evolution of vertices inside watershed lines, we prevent also the model to minimize its energy around watershed lines. Thus, we propose to combine DSM-Balloon and watershed algorithm to provide an explicit way to compute smooth minimal surfaces.

Our basic assumption, DSM with watershed combination, is that the surface to be computed is embedded in the watershed segmentation images. This proposition is motivated by two observations. Firstly, the watershed lines contain all major boundaries of real images which can alleviate the convergence and initialization problem. Secondly, DSM-Balloon is able to overcome the watershed over-segmentation and smoothness problem and can interpolate messing data between slices. Thus, we propose to solve the following combinatorial problem: finding a surface composed of a finite union of watershed lines such that DSM-Balloon minimizes a given geometric functional.

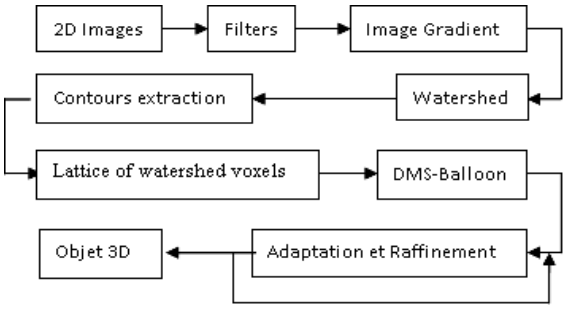

Fig. 7: combined DSM-Balloon and watershed diagram.

The method consists in the first phase to segment each image. Once a set of slices has been segmented with watershed, it becomes necessary to map the result to tri-dimensional space (Lattice of watershed voxels). Watershed lattice serves to initialize, in preliminary stage, DSM-Balloon. The initial mesh undergoes rigid and affine transformations that place mesh as accurately as possible over the watershed lines. After this step, the mesh progressively begins to undergo globally-constrained deformations, which allow it to adapt itself to smaller variations of watershed lines. The mesh deformation, over watershed lattice voxels, is concretely different to deformation process of original simplex meshes reconstruction algorithm.

4. RESULTS

We estimate the volume of heart left ventricle LV to compare the previously cited models. In this paper, LV reconstruction doesn't take into account the heart dynamics, that is, the volumetric variation sequence of the heart during the time. Our objective is to reconstruct the LV at the end of systole and at the end of diastole.

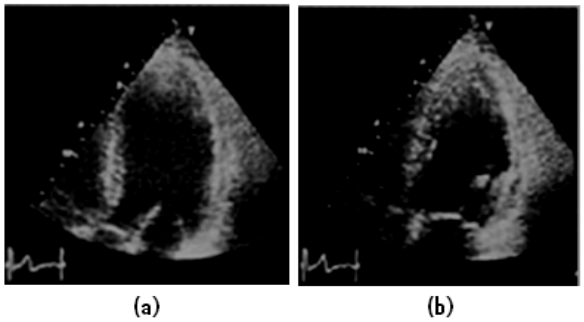

Fig. 8: (a) the end of systole "contraction" and (b) the end of diastole" dilation ".

The method proposed through our system is consistent and regular. The combined results of DSM-Balloon and watershed are given in (Fig. 10 and Fig. 11). As observed in the results, our method has two advantages. The first one is the ability to inflate and deflate the deformable simplex mesh which prevents vertices negative transitions. Thus, wrong boundary extraction. The second important advantage: this approach alleviates the convergence problem and allows a closely automatic initialization of the simplex meshes. The initialization is based on the knowledge acquired with watershed segmentation, which is often practical when segmenting complex 3D objects.

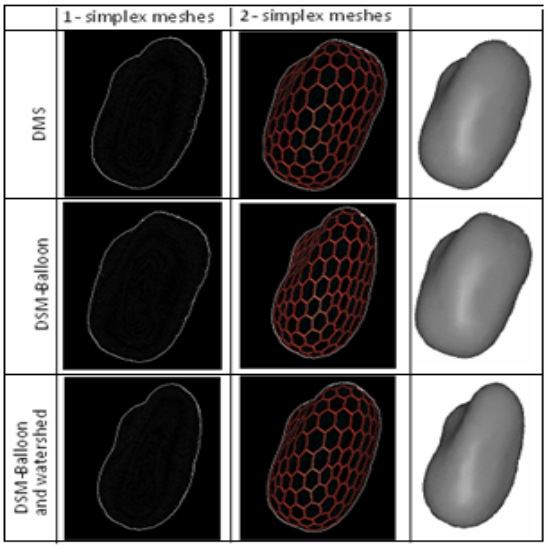

Fig. 9: (End of systole) Reconstruction results of LV with the DSM, and combined watershed with DSM-Balloon respectively with 1 and 2-simplex meshes.

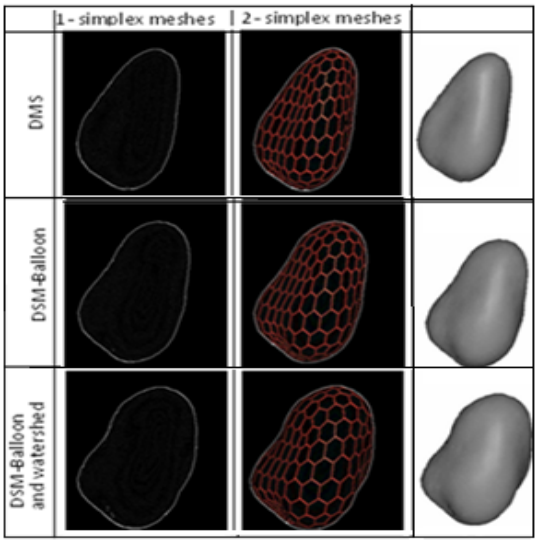

Fig. 10: (end of diastole) Reconstruction results of LV with the DSM, and combined watershed with DSM-Balloon respectively with 1 and 2-simplex meshes.

5. CONCLUSION

Generally, the mesh closeness to modelled object depends on the number of its vertices, the distance of vertices to the data and the relative location of vertices on the surface object

DSM-balloon increases the likelihood to fit the valid boundaries and the surface energy minimisation. Thus, improve valid missing data interpolation. The efficient knowledge extracted by watershed from 2D images is used to generate meaningful constraints deformation rules and to write new guidelines to improve outcomes of DSM-Balloon. By incorporating watershed knowledge as prior information about the object shape, our proposed system combines the benefits of deformable simplex meshes and the robustness of watershed based method. Indeed, the proposed hybrid method allows overcoming the poor convergence and initialization problem of DSM-balloon.

REFERENCES

[1] Kass M, Witkin A, Terzopoulos D. 1987. Snakes: active contour models. Int J Comput Vision 1:321–331, 1987.

[2] Malladi R, Sethian JA, Vemuri BC. Shape modeling with front propagation: a level set approach. IEEE Trans Pattern Anal Machine Intell 17(2):158–175, 1995

[3] Caselles V, Catte F, Coll T, Dibos F. 1993. A geometric model for active contours in image processing. Num Math 66:1–32, 1993

[4] Leymarie F, Levine MD. Tracking deformable objects in the plane using an active contour model. IEEE Trans Pattern Anal Machine Intell 15:617–634, 1993.

[5] Durikovic R, Kaneda K, Yamashita H. Dynamic contour: a texture approach and contour operations. Visual Comput 11:277–289, 1995.

[6] Terzopoulos D. The computation of visible-surface representations. IEEE Trans Pattern Anal Machine Intell 10(4):417–438, 1988.

[7] Terzopoulos D, Szeliski R. Tracking with Kalman snakes. In Active vision, pp. 3–20. Ed A Blake, A Yuille. Cambridge: MIT Press, 1992.

[8] Delingette H. General object reconstruction based on simplex meshes. Int J Computer Vision; 32:111–146, 1999.

[9] L. D. Cohen. On active contour models and balloons. CVGIP-IU, 53(2):211–218, 1991.

[10] K. EL Fazazy, K. Satori. Combined watershed and deformable simplex mesh for volumetric reconstruction. IJCSNS, VOL.9 No.9, September 2009

[11] Beucher, S. Watershed, hierarchical segmentation and waterfall algorithm. In Mathematical Morphology and its Applications to Image Processing, J. Serra and P. Soille, Eds. Kluwer Acad. Publ., Dordrecht, 1994, pp. 69-76.

[12] Meyer, F., and Beucher, S. Morphological segmentation. J. Visual Commun. and Image Repres. 1,1 (1990), 21-45.

[13] Beucher, S., and Lantuéjoul, C. Use of watersheds in contour detection. In Proc. International Workshop on Image Processing, Real-Time Edge and Motion Detection/Estimation, Rennes, September (1979).

[14] Beucher, S., and Meyer, F. The morphological approach to segmentation: the watershed transformation. In Mathematical Morphology in Image Processing, E. R. Dougherty, Ed. Marcel Dekker, New York, 1993, ch. 12, pp. 433-481.

[15] Meyer, F. Topographic distance and watershed lines. Signal Processing 38 (1994), 113-125.

[16] Vincent, L. Algorithmes Morphologiques a Base de Files d'Attente et de Lacets. Extension aux Graphes. PhD thesis, Ecole Nationale Supérieure des Mines de Paris, Fontainebleau, 1990.

[17] Vincent, L., and Soille, P. Watersheds in digital spaces: an efficient algorithm based on immersion simulations. IEEE Trans. Patt. Anal. Mach. Intell. 13, 6 (1991), 583-598.

BIOGRAPHY

El Fazazy Khalid received the bachelor's degrees from Faculty of Sciences USMBA Fez in 1999 and master's degrees from ENSA-Tanger in 2004. He is currently working toward the PhD degree in the LIIAN Laboratory at USMBA-Fez University. His current research interests include medical image analysis and 3D object reconstruction.

Khalid Satori received the PhD degree from the National Institute for the Applied Sciences INSA at Lyon in 1993. He is currently a professor of computer science at Faculty of Sciences USMBA Fez. He is the director of the LIIAN Laboratory. His research interests include real time rendering, Image-based rendering, virtual reality, biomedical signal, camera self-calibration and 3D reconstruction.